Acta Crystallographica Section B
Structural Science
ISSN 0108-7681

Intermolecular interactions and charge transfer in the 2:1 tetrathiafulvalene bromanil complex, $(TTF)_2$-BA

Pilar García-Orduña,[a,b] Slimane Dahaoui[a]* and Claude Lecomte[a]

[a]Laboratoire de Cristallographie, Résonance Magnétique et Modélizations (CRM2) UMR CNRS-UHP 7036, Institut Jean Barriol, Université Henri Poincaré, BP 70239, 54506 Vandoeuvre-les-Nancy, France, and [b]Departamento de Química Inorgánica, Instituto de Síntesis Química y Catálisis Homogénea (ISQCH), Universidad de Zaragoza CSIC, 50009 Zaragoza, Spain

Correspondence e-mail: slimane.dahaoui@crm2.uhp-nancy.fr

Received 16 December 2010
Accepted 26 April 2011

The crystal structure of the 2:1 charge-transfer complex of tetrathiafulvalene [2,2′-bis(1,3-dithiolylidene)] and bromanil (tetrabromo-1,4-benzoquinone) [$(TTF)_2$-BA, $(C_6H_4S_4)_2$–$C_6Br_4O_2$] has been determined by X-ray diffraction at room temperature, 100 and 25 K. No structural phase transition occurs in the temperature range studied. The crystal is made of TTF–BA–TTF sandwich trimers. A charge-transfer estimation between donor and acceptor (0.2 e) molecules is proposed in comparison to the molecular geometries of TTF–BA and TTF and BA isolated molecules. Displacement parameters of the molecules have been modeled with the TLS formalism.

1. Introduction

Understanding strong and weak interatomic interactions enables the design and manipulation of molecular systems whose physical properties depend on crystal packing. The importance of such a study is shown by many examples, such as organic charge-transfer (CT) complexes which are built by co-crystallization of organic planar electron donor (*D*) and acceptor (*A*) molecules, often aromatic rings. The properties of these complexes depend on their crystal packing which drives the interactions between *D* and *A* to control the charge transfer. Most studies concern 1:1 charge-transfer complexes in which *D* and *A* form segregated (...–*D*–*D*–*D*–... ...–*A*–*A*–*A*–...) or mixed (...–*D*–*A*–*D*–...) stacks. The former generally present a high electric conductivity in the direction of stacking (Cohen *et al.*, 1974). The latter are usually insulators or semiconductors at ambient conditions. Some of them undergo an unusual phase transition, called a neutral–ionic phase transition, related to the variation of the partial degree of charge transfer (q_{TC}; Torrance & Mayerle, 1981; Le Cointe *et al.*, 1995; García *et al.*, 2007). This phase transition is accompanied by structural modifications of the stacking, most often with symmetry breaking, with the formation of *D*–*A* pairs. We have recently shown the possibility of characterizing the two microscopic control parameters (dimerization and charge transfer) *via* experimental charge-density studies (García *et al.*, 2007).

By applying temperature, pressure and light excitation charge transfer may also be induced in 2:1 molecular complexes, but no structural evidence has been published yet. Previous studies concerned pressure evolution of the ionicity of the *D* and *A* molecules from spectroscopic studies: it has been proposed that ionicity increases with pressure (Matsuzaki *et al.*, 1992; Tasaki *et al.*, 1997), and a non-uniform charge distribution between two moieties of the *D*–*A*–*D* trimer was deduced from electron-molecular vibration coupling (Matsuzaki & Yartsev, 1994; Basaki *et al.*, 1997). Moreover, this non-uniform charge distribution has also been observed on *A* sites,

Table 1
Experimental details.

For all structures: $2C_6H_4S_4{\cdot}C_6Br_4O_2$, M_r = 416.20, monoclinic, $P2_1/n$, Z = 4. Experiments were carried out with Mo $K\alpha$ radiation using an Xcalibur-Saphire2 diffractometer. Absorption: integration using *ABSORB* (DeTitta, 1985). Refinement was on 145 parameters with 0 restraints. H-atom parameters were not refined.

	293 K	100 K	25 K
Crystal data			
a, b, c (Å)	10.3653 (7), 11.7998 (7), 11.0749 (7)	10.2781 (9), 11.5982 (8), 11.0418 (9)	10.2507 (6), 11.5276 (9), 10.9799 (9)
β (°)	110.217 (6)	110.434 (8)	110.446 (7)
V (Å^3)	1271.10 (14)	1233.44 (17)	1215.71 (15)
μ (mm^{-1})	7.01	7.22	7.33
Crystal size (mm)	0.40 × 0.40 × 0.20	0.40 × 0.40 × 0.20	0.40 × 0.40 × 0.20
Data collection			
T_{min}, T_{max}	0.113, 0.236	0.086, 0.282	0.009, 0.233
No. of measured, independent and observed [$I > 2\sigma(I)$] reflections	18 082, 3761, 2563	51 302, 3972, 3905	48 219, 3936, 3775
$(\sin\theta/\lambda)_{max}$ (Å^{-1})	0.727	0.727	0.727
Completeness (%)	92	99	99
$R[F^2 > 2\sigma(F^2)]$, $wR(F^2)$, S	0.038, 0.105, 0.99	0.033, 0.083, 1.12	0.025, 0.067, 1.10
No. of reflections	3761	3761	3936
$\Delta\rho_{max}$, $\Delta\rho_{min}$ (e Å^{-3})	0.71, −0.68	1.31, −0.70	0.96, −0.82

Computer programs used: *KappaCCD* (Nonius, 1998), *DENZO* and *SCALEPAK* (Otwinowski & Minor, 1997), *CrysAlis* (Oxford Diffraction Ltd, 2010), *SHELXS*97, *SHELXL*97 (Sheldrick, 2008), *ORTEP*III (Farrugia, 1997), *WinGX* publication routines (Farrugia, 1999).

suggesting that coupled trimers may behave cooperatively (Sadohara & Matsuzaki, 1997).

Therefore, it is essential to characterize the intermolecular interactions which occur in these complexes. In the present study we analyzed the evolution of the crystal structure of the 2:1 charge-transfer complex of tetrathiafulvalene and bromanil [$(TTF)_2$-BA, $(C_6H_4S_4)_2$–$C_6Br_4O_2$] from 25 K to room temperature as measured by accurate single-crystal X-ray diffraction. Donor (TTF) and acceptor (BA) molecules are represented below.

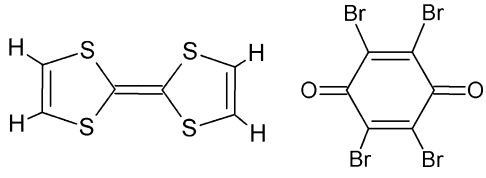

2. Experimental

2.1. TTF_2-BA crystallization

TTF and BA powders were purchased from Lancaster and purified. Single crystals of $(TTF)_2$-BA were grown by sublimation of the component materials in a vacuum-sealed Pyrex glass tube, which was placed in a specially designed homemade electrical furnace, with two coils. This allows the two compounds to be heated at two different temperatures, T_1 = 388 K and T_2 = 352 K, which are the sublimation temperatures of BA and TTF, respectively. After 2 weeks dark prismatic-like crystals were obtained.

2.2. X-ray crystallography

The temperature evolution of the unit-cell parameters between 100 and 293 K was studied by single-crystal diffraction on an Xcalibur-Saphire2 CCD Oxford Diffraction diffractometer, with Mo $K\alpha$ radiation. The crystal was cooled using an Oxford Cryostream N_2 open-flow cryostat. The unit-cell parameters were determined from the analysis of diffracted intensities on the same 20 images, with a fixed detector position and four different values for φ. The unit-cell parameter evolution is given in Fig. S1 (supplementary material[1]) and does not show any structural phase transition.

The crystal structure X-ray diffraction data were collected at 293, 100 and 25 K. An Oxford–Helijet open-flow He gas cryostat was used for the 25 K experiment. Images were collected at a fixed detector position using 115° ω step scans repeated at 4 different φ angle values. The 100 and 25 K diffraction data were collected for a charge-density analysis which explains the number of measured data; however, their quality was not good enough for a physically meaningful electron-density model. The lower number of data collected at 25 K accounts for geometrical limitations due to the He blower during data collection.

Data processing was performed using the *CrysAlis Red* program (Oxford Diffraction Ltd, 2010). Absorption was corrected for by numerical methods based on crystal-faces indexing with *ABSORB* (DeTitta, 1985). Such a correction was deemed necessary to obtain reliable data (T_{min} = 0.086, T_{max} = 0.282, see Table 1); it may be surprising that T_{min} and T_{max} are different from one experiment to another, but it is in line with the number of reflections collected. In the room-temperature study the total number of collected data is much smaller and the angular conditions of the reciprocal lattice nodes to enter the Ewald sphere are not the same, and consequently the incoming and diffraction optical pathways depend on the experiment. Reflections having $I > 2\sigma(I)$ were used. The structures were solved by direct methods (Sheldrick,

[1] Supplementary data for this paper are available from the IUCr electronic archives (Reference: GW5013). Services for accessing these data are described at the back of the journal.

Table 2
TTF and BA bond lengths (Å) in TTF (García *et al.*, 2007), BA (García-Orduña *et al.*, 2011), TTF-BA (García *et al.*, 2005) and TTF_2-BA at 100 K and TTF-CA at 105 K (García *et al.*, 2007).

Bond lengths in TTF and TTF-BA crystals correspond to mean bond lengths of the independent molecules of the unit cell.

	TTF	BA	TTF-CA	TTF-BA	$(TTF)_2$-BA
C═$C_{central}$	1.340 (4)	–	1.3678 (7)	1.398 (4)	1.360 (3)
C−$S_{central}$	1.765 (7)	–	1.7497 (4)	1.725 (3)	1.760 (4)
C−S	1.752 (5)	–	1.7423 (5)	1.729 (3)	1.746 (4)
C═C	1.322 (3)	–	1.7500 (4)	1.338 (4)	1.346 (4)
C═C	–	1.343 (2)	–	1.462 (4)	1.358 (3)
C−C	–	1.491 (2)	–	1.371 (3)	1.493 (3)
C═O	–	1.217 (2)	–	1.241 (4)	1.229 (3)
C−Br	–	1.8615 (15)	–	1.887 (3)	1.878 (3)

2008) and successive Fourier synthesis, and then refined by full-matrix least-square refinements against F^2 using the *SHELXL*97 program (Sheldrick, 2008). All non-H atoms were refined anisotropically. H atoms were observed in Fourier maps, then refined riding on their attached atoms with isotropic displacement parameters fixed at 1.2 times the U_{eq} of the attached atoms. The type of space group does not change and no discontinuity is observed on the metric of the unit cell, from 293 to 25 K, confirming that no phase transition occurs, contrary to TTF-CA [tetrathiafulvalene chloranil (tetrachloro-1,4-benzoquinone) complex]. The asymmetric unit contains one TTF molecule and half a bromanil, which lies on the ($\frac{1}{2}$ 0 0) inversion center of the $P2_1/n$ space group. All atoms are on general positions. The final positions and displacement parameters are given in the supplementary material together with all the geometrical parameters. Further details on the crystal data and experimental conditions are given in Table 1.

3. Results and discussion

No mixed or segregated stack is observed in $(TTF)_2$-BA in contrast to the 1:1 complex (García *et al.*, 2005); in this crystal structure the building block is a trimer. The packing mode is more similar to the sandwich herringbone structure defined by Gavezzotti & Desiraju (1988) and Desiraju & Gavezzotti (1989) for aromatic hydrocarbons than to the typical arrangement of charge-transfer complexes, where *D* and *A* form mixed or segregated stacks. In $(TTF)_2$-BA the special disposition in orthogonal trimers produces layers, almost parallel to the (101) plane, as shown in Fig. 1. Thus, in these layers each bromanil molecule is surrounded by four TTF molecules: two TTF molecules of the trimer and two others belonging to two orthogonal neighboring trimers. The resulting motif is a cage centered on the BA molecule (Fig. 2).

The relative disposition of the donor and acceptor molecules of the trimer is characteristic of TTF and benzoquinone charge-transfer complexes (Frankenbach *et al.*, 1991) or of complexes substituted benzoquinones like the chloranil (Mayerle & Torrance, 1981), bromanil (García *et al.*, 2005) and fluoranil (Mayerle & Torrance, 1981). The longest axes of each molecule are rotated out of alignment. This rotation between donor and acceptor molecules allows stabilization to be achieved in the overlap of the HOMO orbital of the donor and the LUMO orbital of the acceptor (overlap that would be forbidden as these orbitals have opposite symmetry; Mayerle & Torrance, 1981). In 1:1 TTF-*A*A charge-transfer complexes (*X* being the halogen atom) the angle between the O···O axis tends to be orthogonal to the longer axis of the TTF molecule when the C−*X*/C═O ratio of bond lengths increases. However, when comparing TTF-BA and $(TTF)_2$-BA, even if this ratio is equal (1.53) for both complexes the angle between the TTF axis and the O···O direction in $(TTF)_2$-BA [111.6 (2)°] is not as close to 90° as those observed for TTF-BA [90.0 (5) and 93.8 (5)°]. We can thus conclude that the overlap between HOMO and LUMO orbitals is not optimal in the trimer. The ground state of the 2:1 complex is thus expected to be less ionic than for TTF-BA ($q_{CT} \simeq 0.9$ e; Girlando *et al.*, 1985; García *et al.*, 2005). This can be geometrically verified by comparing the crystal structures of TTF and BA (in each case neutral molecules) with those in 1:1 and 2:1 complexes. Analogous to chloranil (Mayerle & Torrance, 1981), the simple C−C bonds of bromanil molecules are related to the lowest unoccupied orbital (LUMO) which is bonding with respect to these bonds, and antibonding with

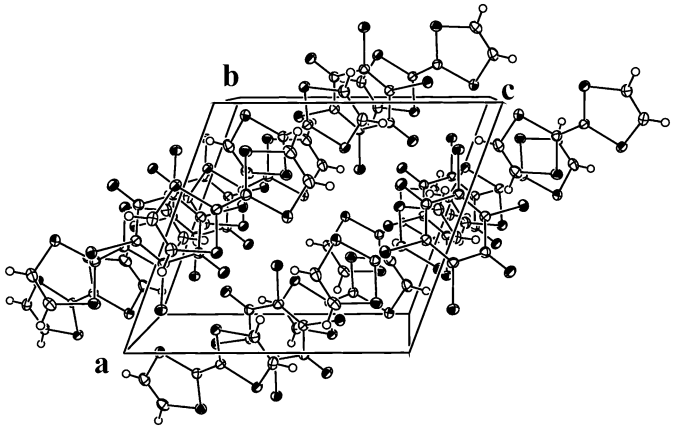

Figure 1
ORTEP view of the unit cell at 100 K, normal to the *b* axis.

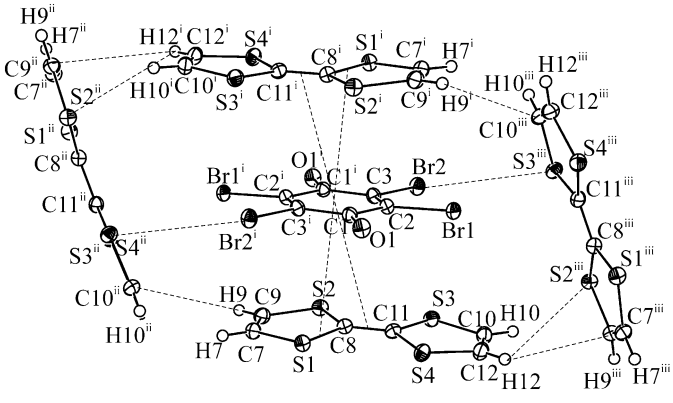

Figure 2
Intermolecular interactions in the cage at 100 K. Symmetry codes: (i) $1-x, -y, -z$; (ii) $\frac{1}{2}-x, -\frac{1}{2}+y, \frac{1}{2}-z$; (iii) $\frac{1}{2}+x, \frac{1}{2}-y, -\frac{1}{2}+z$.

Table 3
Intermolecular interactions (Å) in the $(TTF)_2$-BA crystal.

	293 K	100 K	25 K
Interactions in the layer			
Interactions in the trimer			
C8—S1···centroid(BA)	3.385 (4)	3.290 (4)	3.260 (4)
Br2···S4	3.753 (4)	3.662 (3)	3.636 (4)
Between the trimers			
Br2···S4^{iii}	3.544 (4)	3.504 (4)	3.486 (4)
Interactions between the layers			
S1^{i}···S2^{iv}	3.298 (4)	3.246 (3)	3.223 (4)
S4···C10^{v}	3.609 (4)	3.514 (3)	3.495 (3)

respect to the double C═C and C═O bonds. Thus, when the molecular charge increases the former should be shorter while the latter should be longer. This tendency is clearly seen when comparing these bond lengths in BA, TTF-BA and $(TTF)_2$-BA crystal structures at the same temperature (100 K). Simple C—C bonds in $(TTF)_2$-BA have values of 1.493 (3) Å, equal (within a standard deviation) to 1.491 (2) Å found in the bromanil molecule in its BA crystal (García-Orduña *et al.*, 2011), opposite to those found in TTF-BA, which means that the C—C bond length is 1.458 (5) Å. The double C═C and C═O bonds behave in the same way with almost equal lengths in BA and $(TTF)_2$-BA crystals (Table 2). The geometric parameters of the TTF molecule are more sensitive to the charge transfer and were used to estimate the q_{CT} charge transfer in the 1:1 complexes (Umland *et al.*, 1988). In the case of the 2:1 charge-transfer complexes, where the charge transfer may involve both TTF molecules, deviation from neutral geometry is expected to be smaller: the central C═C bond length [1.354 (4) Å at 100 K] is slightly longer than the corresponding one in the TTF crystal [1.340 (4) Å], and much shorter than those in TTF-BA [1.400 (4) and 1.397 (4) Å]. This small variation of the C═C bond length may be related to the partial charge transfer (q_{CT}) in the complex. The HOMO of TTF is π-bonding with respect to this bond, thus when q_{CT} increases the C═C bond length should increase (Katan, 1999). An approximate charge transfer of 0.2 e can then be evaluated from both the ratio (r/s) and the difference ($r - s$) of TTF geometric parameters for $(TTF)_2$-BA in the whole temperature range studied (see Umland *et al.*, 1988, for definitions of the r and s parameters). Hence, the central C═C bond length of the TTF molecule in the trimer does not change with temperature [1.354 (4), 1.360 (3) and 1.360 (3) Å at 293, 100 and 25 K, respectively]. Thus, based on this criteria used by all authors when no charge-density study is available, the molecules seem to be partially charged between 25 K and room temperature, and the resulting complex may be written as $(TTF^{0.2+})_2BA^{0.4-}$. This assumption is in line with the non-planarity of the TTF molecule. Deviation of the non-H atoms from the mean plane of the molecule for the three studied temperatures is reported in the supplementary material. TTF is a very flexible molecule whose conformation depends on the intermolecular interactions in the crystal. At room temperature the largest displacement from the mean plane defined by the non-H atoms [0.060 (3) Å] is observed for the central C8 atom. This value increases to 0.085 (2) and 0.0915 (2) Å at 100 and 25 K. In the TTF-BA structure all non-H atoms of TTF are coplanar within ±0.012 (1) and ±0.028 (1) Å in high- and low-temperature phases. In the trimer the bending angle (*i.e.* the dihedral angle between each cycle of the molecule) is 4.9 (1)° at room temperature and reaches 6.8 (1) and 7.3 (1)° at 100 and 25 K. The torsion angles around the central C═C bond also reflect the distortion of the molecule: S2—C8—C11—S3 and S4—C8—C11—C1 are not similar [−2.0 (4) and −0.7 (4)°] at room temperature, and the difference is larger at 25 K [−3.5 (2) and 0.0 (2)°]. These geometrical parameters indicate that the TTF molecule is more distorted than those observed in the TTF-BA dimer units.

Therefore, when $(TTF)_2$-BA is formed the major geometrical changes concern the TTF molecule, contrary to TTF-BA and TTF-CA complexes; it leads to an estimated charge transfer of q_{CT} = 0.2 e from each TTF, compared with 0.9 e in TTF-BA and 0.74 (2) e in the antiferroelectric TTF-CA phase (García *et al.*, 2007). The resulting estimated BA charge (0.4 e) does not seem to strongly affect its geometry. Furthermore, joint experimental and theoretical accurate charge-density studies of TTF-BA and $(TTF)_2$-BA followed by a Bader partitioning (Bader & Essén, 1984) should give a definitive answer about q_{CT} and its relation to the geometry of *X*A molecules.

Several other geometrical features point to the strong connection between donor and acceptor molecules in the trimer. Donor and acceptor molecules are not parallel, their mean planes form a dihedral angle of 3.20 (8)°, very close to that observed for TTF-CA 3.0° and smaller than those found in TTF-FA, 4.2° (Mayerle *et al.*, 1979), and TTF-BA, 5.5 (5) and 4.1 (6)° (García *et al.*, 2005). When cooling, this dihedral angle remains constant but molecules become closer in line with the thermal contraction of the unit cell. The dimensions of the cage (Fig. 2), estimated from the distance between the TTF and BA molecule centers, decrease from 7.38 (3) × 13.78 (3) Å^2 at room temperature to 7.23 (3) × 13.69 (3) Å^2 and 7.18 (3) × 13.64 (3) Å^2 at 100 and 25 K.

Intermolecular interactions in the cage are shown in Fig. 2 and their geometrical parameters are summarized in Table 3. The stronger contact in the trimer takes place between the π-electrons of the benzene ring and the C8—S1 bond of the TTF molecule. In the stacking direction and between orthogonal trimers in the layer, intermolecular interactions between bromine and sulfur occur: at room temperature the Br2···S4^{iii} [symmetry code (iii) $\frac{1}{2}+x, \frac{1}{2}-y, -\frac{1}{2}+z$] distance is 3.544 (4) Å, shorter than the intratrimer Br2···S4 distance, 3.753 (4) Å, and remarkably shorter than the sum of van der Waals radii (3.80 Å). All these contacts (not very common in the literature) depend on temperature, the distances decreasing from 3.544 (4) and 3.753 (4) to 3.486 (4) and 3.636 (4) Å when cooling from 293 to 25 K. Thus, the bromanil molecule is trapped between the four TTF molecules.

Besides all these interactions in the (010) plane the supramolecular architecture of the complex is based on hydrogen bonds and van der Waals interactions between S atoms of TTF

Table 4
T and **L** tensors of the bromanil molecule in $(TTF)_2$-BA at 100 K, referred to as the inertial system axis.

T ($\times 10^{-4}$ Å^2)			**L** (deg^2)		
158 (3)	3 (3)	−14 (4)	4.7 (4)	1.1 (1)	−0.5 (3)
	153 (2)	3 (3)		1.3 (2)	−0.1 (2)
		166 (5)			2.1 (2)

molecules belonging to other layers, as seen in Fig. 3. Intermolecular interactions are given in the supplementary material. S···S contacts are characteristic of TTF derivatives; hence it has been considered to be an important structural element that facilitates electrical conductivity (Wudl *et al.*, 1972; Ferraris *et al.*, 1973; Bryce, 1991; Yamashita *et al.*, 1996). At room temperature the $S1^{i}\cdots S2^{iv}$ distance is 3.298 (4) Å, remarkably shorter than the sum of van der Waals radii (3.60 Å), and similar to that observed in the mixed-stack bis(ethylenedithio)tetrathiafulvalene 2,5-dimethyltetracyanoquinodimethane (BEDTTF-Me_2TCNQ; $C_{10}H_8S_8$–$C_{14}H_8N_4$), 3.299 Å. This intercolumnar interaction in BEDTTF-Me_2TCNQ is comparable to those between *D* and *A* molecules along the mixed stack, as pointed out by Hasegawa *et al.* (2000). In $(TTF)_2$-BA this S···S contact is mainly along the [101] direction, and therefore the thermal contraction in this direction is not favorable. This result agrees with the anisotropy observed in the principal linear thermal expansion/contraction coefficients (see Fig. S1, supplementary material): α_b (10.1×10^{-5} K^{-1}) being much larger than the other thermal coefficients, α_a and α_c, 5.7 and 1.8×10^{-5} K^{-1}. This large coefficient α_b is related to the interactions along the stack and may explain the distortion of the TTF planarity, as already discussed.

Results of the thermal motion analysis (Dunitz *et al.*, 1988; Schomaker & Trueblood, 1998) of the bromanil molecule in the complex, in relation to the inertial system axis, are summarized in Table 4. For clarity, only the **T** and **L** tensors at 100 K are reported. **T** and **L** tensors at room temperature and 25 K, as well as those of the TTF molecule are given in the supplementary material. At 100 K the **T** tensors of TTF and BA molecules are almost isotropic (0.0160 ± 0.0006 Å^2). The bromanil molecule is trapped and coupled to four TTF molecules, as discussed before. The occurrence of a phase transition involving the loss of the bromanil inversion center would imply the displacement of the molecule in a specific direction out of the layer which cannot be foreseen from this TLS model. This may explain the stability of the studied phase *versus T*.

Finally, if the TLS parameters of TTF and BA molecules in their crystal structures are compared with those of the 1:1 and 2:1 complexes, we note that:

(i) translation is always isotropic;

(ii) the principal axes of libration of the molecules do not change when forming the charge-transfer complexes;

(iii) the main difference is the amplitude of the BA libration in the trimer (4.8 deg^2, at 100 K) which is much lower than that in TTF-BA where BA molecules have a principal libration of 14.8 and 12.8 deg^2.

4. Conclusions

The structures of the 2:1 charge-transfer complex $(TTF)_2$-BA at room temperature, 100 and 25 K have been reported. TTF and BA molecules form a herringbone packing, with orthogonal trimer units yielding layers parallel to the (101) plane. Thermal displacement analysis has been performed. Comparison with those of the isolated molecules and the 1:1 charge-transfer complex at 100 K revealed that libration is smaller in the 2:1 complex, where translation of TTF and BA molecules is isotropic and quite similar. Consequently, the donor and acceptor are strongly coupled. This observation agrees with the molecular geometry, where the distortion of the TTF molecule has been shown. The TTF bond lengths indicate the existence of a partial charge transfer of 0.2 e that remains constant with temperature. On the contrary, the BA geometry suggests that the molecule remains neutral in the complex. Therefore, an accurate charge estimation is needed by using DFT calculations and high-energy synchrotron data for precise experimental density studies followed by a Bader topological analysis.

Thermal contraction enhances the Br···S interactions inside and between the trimers, in a very close-packing mode. In the [101] direction the crystal cohesion is held in place by remarkably short S···S contacts. These close contacts prevent the possibility of the existence of a phase transition with symmetry breaking.

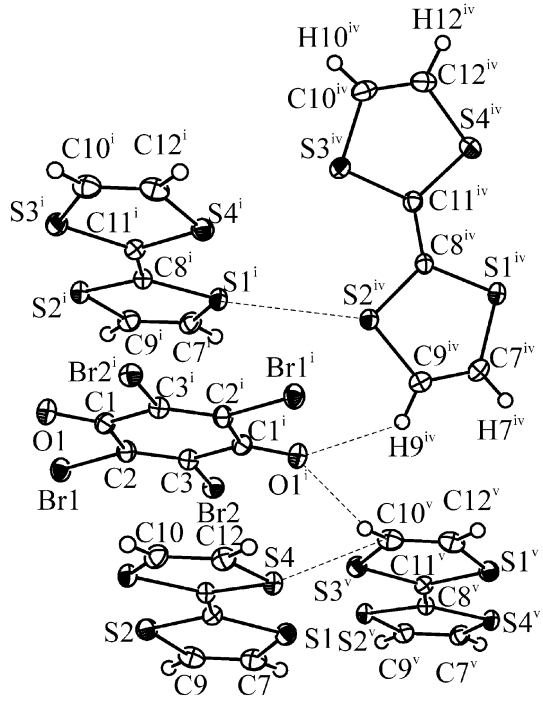

Figure 3
Intermolecular interactions between the layers. Symmetry codes: (i) $1-x, -y, -z$; (iv) $\frac{3}{2}-x, -\frac{1}{2}+y, \frac{1}{2}-z$; (v) $1-x, -y, 1-z$.

The authors thank the Service Commun de Diffraction X sur Monocristaux (Université Henri Poincaré, Nancy 1) for providing access to crystallographic experimental facilities. We would also cordially thank A. Bouché for the crystal synthesis. Authors are indebted to Oxford Diffraction for lending for free the Oxford-Helijet cryostat used for the 25 K diffraction measurements. PGO acknowledges financial support from the CSIC, '*JAE-Doc*' program, contract co-funded by the ESF.

References

Bader, R. F. W. & Essén, H. (1984). *J. Chem. Phys.* **80**, 1943–1960.
Basaki, S., Matsuzaki, S. & Yartsev, V. (1997). *Phys. B*, **239**, 171–175.
Bryce, M. R. (1991). *Chem. Soc. Rev.* **20**, 355–390.
Cohen, M. J., Coleman, L. M., Saito, A. F. & Heeger, A. J. (1974). *Phys. Rev. B*, **10**, 1298–1307.
Desiraju, G. R. & Gavezzotti, A. (1989). *J. Chem. Soc. Chem. Commun.* **10**, 621–623.
DeTitta, G. T. (1985). *J. Appl. Cryst.* **18**, 75–79.
Dunitz, J. D., Maverick, E. F. & Trueblood, K. N. (1988). *Angew. Chem. Int. Ed. Engl.* **27**, 880–895.
Farrugia, L. J. (1997). *J. Appl. Cryst.* **30**, 565.
Farrugia, L. J. (1999). *J. Appl. Cryst.* **32**, 837–838.
Ferraris, J., Cowan, D. O., Walatka, V. V. & Perlstein, J. H. (1973). *J. Am. Chem. Soc.* **95**, 948–949.
Frankenbach, G. M., Beno, M. A. & Williams, J. M. (1991). *Acta Cryst.* C**47**, 762–764.
García, P., Dahaoui, S., Fertey, P., Wenger, E. & Lecomte, C. (2005). *Phys. Rev. B*, **72**, 104115.
García, P., Dahaoui, S., Katan, C., Souhassou, M. & Lecomte, C. (2007). *Faraday Discuss.* **135**, 217–235.
García-Orduña, P., Dahaoui, S. & Morgenroth, W. (2011). Submitted.
Gavezzotti, A. & Desiraju, G. R. (1988). *Acta Cryst.* B**44**, 427–434.
Girlando, A., Pecile, C. & Torrance, J. B. (1985). *Solid State Commun.* **54**, 753–759.
Hasegawa, T., Mochida, T., Kondo, R., Kagoshima, S., Iwasa, Y., Akutagawa, T., Nakamura, T. & Saito, G. (2000). *Phys. Rev. B*, **62**, 10059–10066.
Katan, C. (1999). *J. Phys. Chem. A*, **103**, 1407–1413.
Le Cointe, M., Lemée-Cailleau, M. H., Cailleau, H., Toudic, B., Toupet, L., Heger, G., Moussa, F., Schweiss, P., Kraft, K. H. & Karl, N. (1995). *Phys. Rev. B*, **51**, 3374–3386.
Matsuzaki, S., Hiejima, T. & Sano, M. (1992). *Solid State Commun.* **82**, 301–304.
Matsuzaki, S. & Yartsev, V. (1994). *Solid State Commun.* **89**, 941–944.
Mayerle, J. J. & Torrance, J. B. (1981). *Acta Cryst.* B**37**, 2030–2034.
Mayerle, J. J., Torrance, J. B. & Crowley, J. I. (1979). *Acta Cryst.* B**35**, 2988–2995.
Nonius (1998). *COLLECT*. Nonius BV, Delft, The Netherlands.
Otwinowski, Z. & Minor, W. (1997). *Methods in Enzymology*, Vol. 276, *Macromolecular Crystallography*, Part A, edited by C. W. Carter Jr & R. M. Sweet, pp. 307–326. New York: Academic Press.
Oxford Diffraction Ltd (2010). *CrysAlis CCD*, Version 1.171.33. Oxford Diffraction Ltd, Abingdon, Oxfordshire, England.
Sadohara, R. & Matsuzaki, S. (1997). *Phys. B*, **239**, 176–180.
Schomaker, V. & Trueblood, K. N. (1998). *Acta Cryst.* B**54**, 507–514.
Sheldrick, G. M. (2008). *Acta Cryst.* A**64**, 112–122.
Tasaki, K., Matsuzaki, S. & Yartsev, V. (1997). *Solid State Commun.* **103**, 365–369.
Torrance, J. B. & Mayerle, J. J. (1981). *Solid State Commun.* **38**, 1165–1169.
Umland, T. C., Allie, S., Kulhlmann, T. & Coppens, P. (1988). *J. Phys. Chem.* **92**, 6456–6460.
Wudl, F., Wobschall, D. & Hufnagel, E. J. (1972). *J. Am. Chem. Soc.* **94**, 670–672.
Yamashita, Y., Tomura, M. & Imaeda, K. (1996). *Chem. Commun.* **17**, 2021–2022.